Rev. Roum. Sci. Techn.– Électrotechn. et Énerg.
Vol. **61**, *4*, pp. 319–324, Bucarest, 2016

DESIGN AND IMPLEMENTATION OF HIGH PERFORMANCE FIELD ORIENTED CONTROL FOR GRID-CONNECTED DOUBLY FED INDUCTION GENERATOR VIA HYSTERESIS ROTOR CURRENT CONTROLLER

FAYSSAL AMRANE[1,*], AZEDDINE CHAIBA[1], BADR EDDINE BABES [1], SAAD MEKHILEF [2]

Key words: Field oriented control (FOC), Doubly fed induction generator (DFIG), Hysteresis current (HC), Rotor side converter (RSC), Three phase locked loop (3PLL), Total harmonic distortion (THD), dSPACE1104, Wind energy conversion system (WECS).

This paper presents the design and real time implementation of a field-oriented control (FOC) for grid-connected variable speed wind turbine based on doubly fed induction generator (DFIG). The proposed method based on a hybrid Hysteresis Current (HC) with field oriented control (FOC) in order to control the rotor side converter (RSC). The grid-connected DFIG is executed using three phase locked loop (3PLL). The experimental test bench is an emulator turbine represented by direct current motor (DCM) which is coupled with the doubly fed induction generator (DFIG). The implementation is realized using dSPACE1104 card below the synchronous speed. The experimental results show high performances in steady and transient states with low THD of stator current injected to the grid (3.7 %), satisfies the IEEE harmonic standard 519 despite the variation of the references. The main advantages of this control are implementation simplicity and lower switching frequency converter.

1. INTRODUCTION

Many installed wind turbines today are equipped with doubly fed induction machine (DFIM). However, most of these machines are connected directly to the network to avoid the presence of converter. The major advantage of this configuration lies in the fact that the power rating of the inverters is around 25–30 % of the nominal generator power [1, 2]. A doubly fed induction generator (DFIG) is the most important generator used for variable-speed wind energy generation. It consists of a wound rotor induction generator (WRIG) with the stator windings directly connected to a three-phase power grid and with the rotor windings mounted to a bidirectional back-to-back insulated gate bipolar transistor (IGBT) frequency converter [3].

The vector control is the most common method used in the DFIG-based wind turbines [4]. Precise steady-state performance and lower converter switching frequency are the advantages of this method. However, it has some disadvantages, such as its dependence on the machine parameters variation due to the decoupling terms [4]. A new modeling approach based on the flux measurement has been proposed in [5] in order to conclude input-to-state stability and convergence to the desired equilibrium. Control strategies of DFIG have been discussed in details in literatures; direct power control (DPC) [5, 6], model predictive direct power control (MPDPC) [7, 8], sliding mode direct power control [9], Sliding mode control [10] and back-stepping control [11]. A schematic diagram of variable speed wind turbine system with a DFIG is shown in Fig.1.

Many researchers focus their studies based on field oriented control (FOC) using linear regulator proportional integrator (PI) in order to control rotor side converter (RSC) as mention in [5, 12–14], by calculating *K*p and *K*i.

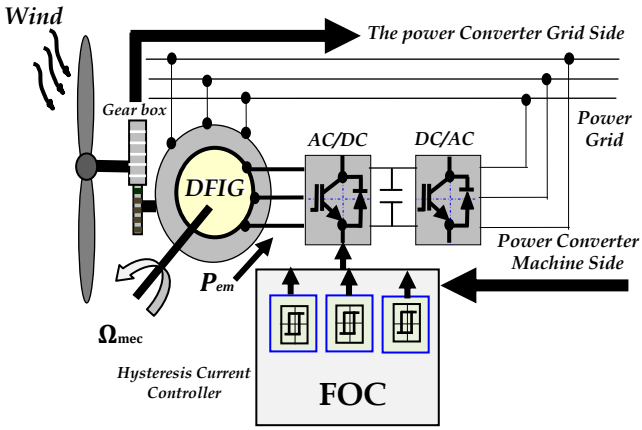

Fig. 1 – Schematic diagram of wind turbine system with a DFIG.

Linear regulator as proportional integrator (PI) needs the full system parameters knowledge and also involve with more computation. While the nonlinear regulator as hysteresis regulator does not need the information about the system parameters and also gives better dynamic response [15]. Most of the researchers in this area are concentrated on analyzing network dynamics, system transients, fault conditions, or grid disturbances [16, 17]. Vector control utilizes the dynamic state relationships of DFIG to define angular speed, amplitude and instantaneous position of current, voltage and flux linkage vectors [18]. In contrast scalar control method, proposition employs steady-state relationships to determine angular speed and amplitude of current, voltage and flux vectors [19]. In [20], the authors propose enhanced hysteresis-based current regulators for vector control DFIG-based wind energy conversion system (WECS), used to control the output currents of the rotor-side and grid-side converters. This proposed hysteresis-based technique has excellent steady-state performances.

[1*] Automatic Laboratory of Setif (LAS), Department of Electrical Engineering, University of Setif 1, 19000 Setif, Algeria. E-mail: amrane_fayssal@live.fr; chaiba_azeddine@yahoo.fr; elect_babes@yahoo.fr
[2] Power Electronics and Renewable Energy Research Laboratory (PEARL), Department of Electrical Engineering, University of Malaya, 50603 Kuala Lumpur, Malaysia. E-mail: saad@um.edu.my

There are two common methods for DFIGs employment in wind power systems such as: stand-alone installation and grid-connected usage. A lot of researches have been performed on doubly fed induction generators operation as grid-connected systems [21]. A new synchronization algorithm for grid connection of a DFIG based on stator flux-oriented vector control for back to-back PWM converters in the DFIG has been proposed by [22]. This method gives fast starting and takes just 2 cycles to be performed and better robustness and has satisfactory performance than existing methods.

In this work, we are interested by the grid-connected usage, because is an appropriate method for large power networks and consequently much researches are in hand in this area, we used the hysteresis current controller to obtain the switching command signals for rotor side converter (RSC). The main contribution in this work is the real time implementation for WECS based on DFIG using hybrid hysteresis current (HC) with field oriented control (FOC). The decoupling terms in control approach is not needed; because the hysteresis controllers have nonlinear nature also we don't use the stator side converter (to minimize the stator power losses).

The purpose of this paper is to build in real time a hybrid field oriented control (FOC) with hysteresis current controller using doubly fed induction generator, to provide good tracking of the predefined references regardless the wind speed changing, and to guarantee converter with unity power factor (zero reactive power), means that the grid side converter (GSC) exchanges only active power with grid.

The rest of this paper is organized as follows; mathematical model of DFIG is presented in Section 2. Section 3 presents the field oriented control of DFIG which is based on the orientation of the rotor flux vector along the axis d. Section 4 presents the topology of hysteresis current controller. The diagram of the implementation is elaborately described in Section 5. In Section 6, experimental results are shown and discussed. Finally, the reported work is concluded in Section 7.

2. MATHEMATICAL MODEL OF DFIG

The general electrical state space model of the induction machine obtained using the Park transformation is given by following equations [23, 24]:

Stator and rotor voltages:

$$V_{sd} = R_s.I_{sd} + \frac{\mathrm{d}}{\mathrm{d}t}\phi_{sd} - \omega_s.\phi_{sq}, \quad (1)$$

$$V_{sq} = R_s.I_{sq} + \frac{\mathrm{d}}{\mathrm{d}t}\phi_{sq} - \omega_s.\phi_{sd}, \quad (2)$$

$$V_{rd} = R_r.I_{rd} + \frac{\mathrm{d}}{\mathrm{d}t}\phi_{rd} - (\omega_s - \omega).\phi_{rq}, \quad (3)$$

$$V_{rq} = R_r.I_{rq} + \frac{\mathrm{d}}{\mathrm{d}t}\phi_{rq} + (\omega_s - \omega).\phi_{rd}. \quad (4)$$

Stator and rotor fluxes:

$$\phi_{sd} = L_s.I_{sd} + L_m.I_{rd}, \quad (5)$$

$$\phi_{sq} = L_s.I_{sq} + L_m.I_{rq}, \quad (6)$$

$$\phi_{rd} = L_rI_{rd} + L_m.L_{sd}, \quad (7)$$

$$\phi_{rq} = L_rI_{rq} + L_mI_{sq}. \quad (8)$$

The electromagnetic torque is given by:

$$C_e = PL_m(I_{rd}I_{sq} - I_{rq}I_{sd}), \quad (9)$$

$$C_e - C_r = J\frac{\mathrm{d}}{\mathrm{d}t}\Omega + f\Omega, \quad (10)$$

$$J = \frac{J_{turbine}}{G^2} + J_g, \quad (11)$$

where ϕ_{sd}, ϕ_{sq} and ϕ_{rd}, ϕ_{rq} are stator and rotor flux components, V_{sd}, V_{sq} and V_{rd}, V_{rq} are stator and rotor voltage components. R_s, R_r are stator and rotor resistances, L_s, L_r are stator and rotor inductances, L_m is mutual inductance, σ is leakage factor, P is number of pole pairs, f is the friction coefficient. C_e, C_r are the electromagnetic and load torque. J, $J_{turbine}$ and J_g are total inertia in DFIG's rotor, inertia of turbine and generator respectively, Ω is mechanical speed and G is gain of gear box.

3. FIELD ORIENTED CONTROL

The DFIG model can be described by the following state equations in synchronous reference frame whose axis d is aligned with the rotor flux vector $(\phi_{rq} = 0)$ and $(\phi_{rd} = \phi_r)$.

$$I_{rq} = -\frac{L_m}{L_r}L_q \quad \text{and} \quad I_{sq} = -\frac{L_r}{L_m}I_{rq}. \quad (12)$$

The arrangement of the equations gives the expressions of the rotor flux and the electromagnetic torque:

$$\phi_{sd} = -\sigma.\frac{L_s.L_r}{L_m}I_{rq}$$

and

$$C_e = PL_m(I_{sq}I_{rd} - I_{sd}I_{rq}) = P\phi_{rd}I_{rq} \quad (13)$$

with $\sigma = 1 - \frac{L_m^2}{L_s.L_r}$.

$$\text{If: } \phi_{sq} = 0 \text{ (via stator)} \equiv \phi_{rd} = L_mL_{sd}. \quad (14)$$

$$\text{If: } I_{sd} = 0 \text{ (via rotor)} \equiv \phi_{rd} = L_rL_{rd}. \quad (15)$$

$$\text{(via stator and rotor)} \equiv \phi_{rd} = L_rL_{rd} + L_mL_{sd}. \quad (16)$$

From equation (13) the rotor reference transversal current is:

$$I^*_{rq} = \frac{Ce^*}{P\phi_{rd}}. \quad (17)$$

4. HYSTERESIS CURRENT CONTROLLER

The two-level hysteresis current control is the simplest non-linear controller which operates by comparing tracking error $e(t)$ with the fixed hysteresis bands ($\pm h$) illustrated in Fig. 2a, where, $e(t)$ is the difference between the reference current $I_{ref}(t)$ and the actual current $I_{act}(t)$ [25–27]. The graphical representation of the two-level hysteresis modulation is shown in Fig. 2b.

$$u(t) = +1 \text{ for } I_{act}(t) < I_{ref}(t) - h \text{ or } e(t) > +h, \quad (18)$$

$$u(t) = -1 \text{ for } I_{act}(t) > I_{ref}(t) + h \text{ or } e(t) < -h. \quad (19)$$

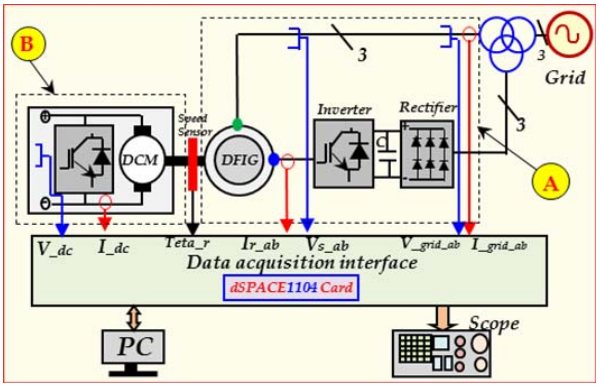

Fig. 2 – Hysteresis current control structure.

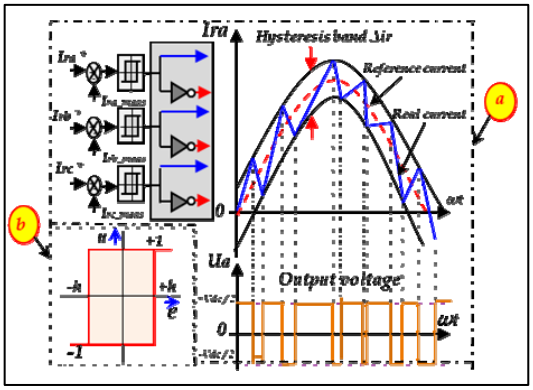

Fig. 4 – Test system.

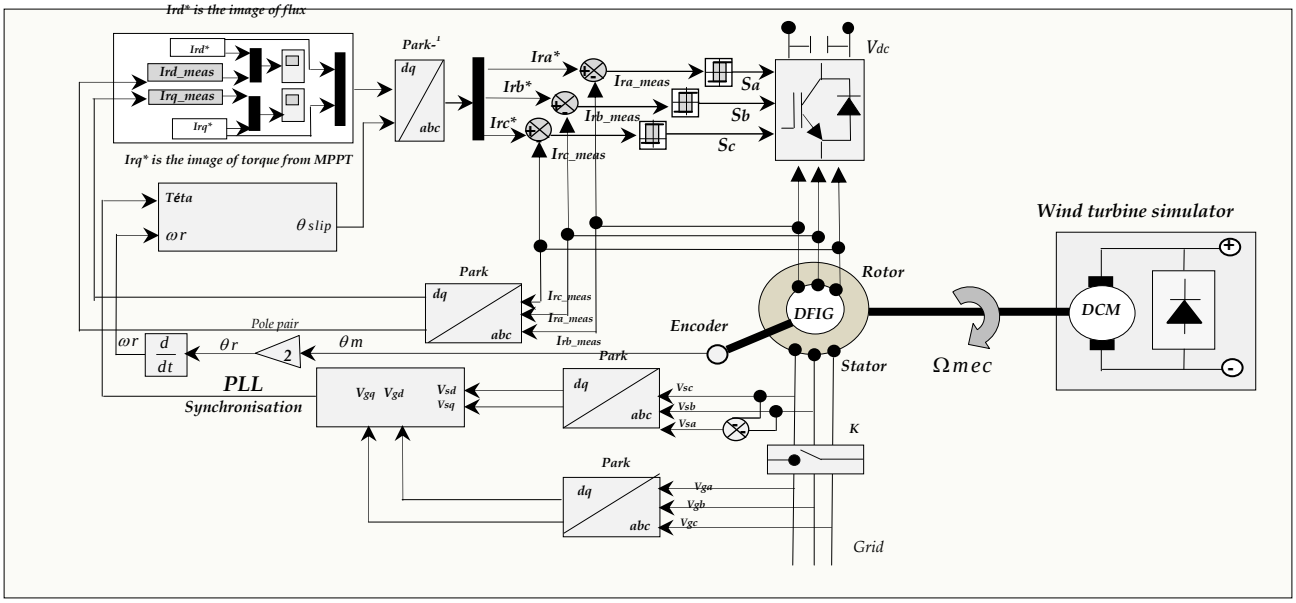

Fig. 3 – Rotor side converter control system.

The rotor side converter (RSC) representing by FOC and hysteresis current topology is illustrated in details in Fig. 3. Stator voltage angle is calculated by using the three phase locked loop (3PLL) algorithm. I^*_{rd} (rotor direct reference current) is the image of flux, and I^*_{rq} (rotor transversal reference current) is the image of torque from is the image of torque from the maximum power point tracking (MPPT).

The grid synchronization control technique and synchronization method have been proposed as this system requires some care during the machine start-up and integration with the grid. The main aim of the synchronization control process is to avoid heavy start-up currents and mechanical stresses on the turbine shaft and other integrated components.

5. STUDY CASE

Figure 4 shows a diagram of wind energy conversion system. In the upper right a is described the DFIG sub-system, composed of a 3.5 kW. And in the upper left b emulator turbine represented by 3 kW direct current motor (DCM).

6. EXPERIMENTAL RESULTS AND DISCUSSION

This is achieved by properly matching the phase angle, frequency, and magnitude of the grid voltage and the stator induced voltage irrespective of whether it is a stator-voltage or stator-flux oriented frame used for modeling the generator. Instead of a traditional control scheme using a phase-locked loop (PLL), the rotor d-q reference current is generated with grid voltage as the reference so as to induce identical voltage in the stator as that of the grid. The machine is started by a driving torque and the switch between stator and the grid can be closed for synchronization. However, appropriate timing of switch closure plays a critical role in satisfying the magnitude condition of synchronization.

Figure 5 presents the experimental test bench for Wind Energy Conversation System (WECS). The DFIG used in this real time implementation is a 3.5 kW (whose parameters are described in Table 1) not designed especially for generation. And direct current motor (DCM) as shown in Figs. 5–9, who's represented wind turbine simulator, to reproduce the aerodynamic torque of a wind turbine. The lower part of Fig. 4 is composed of a data acquisition system connected to the control board. The FOC algorithm is implemented on real time board (dSPACERTI1104) from Texas Instrument with a TMS320F240 DSP (20 MHz) and a microprocessor Power PC 603e (250 MHz); with a

sampling time (fixed step); the controller is executed at 20 kHz. The connections between the dSPACE1104 card and the power converter are carried out by an interface card, which adapts the control signal levels. The current and voltage are ensured by the (Fluke i30S) and (ST1000-II) sensors, whereas, both the rotor position and speed are given by a 1024-pulse incremental encoder implemented on the dc motor shaft (as shown in Fig. 3). After having synchronized and connected the DFIG to the grid using PLL (phase locked loop). Several tests have been carried out to study the performance of the supply-side converter in both transient and steady-state conditions, including bidirectional power flow with lagging, leading and a unity displacement factor. The results are given showing the step-current response for the DFIG for sub- operation (or hypo-synchronous), as follows.

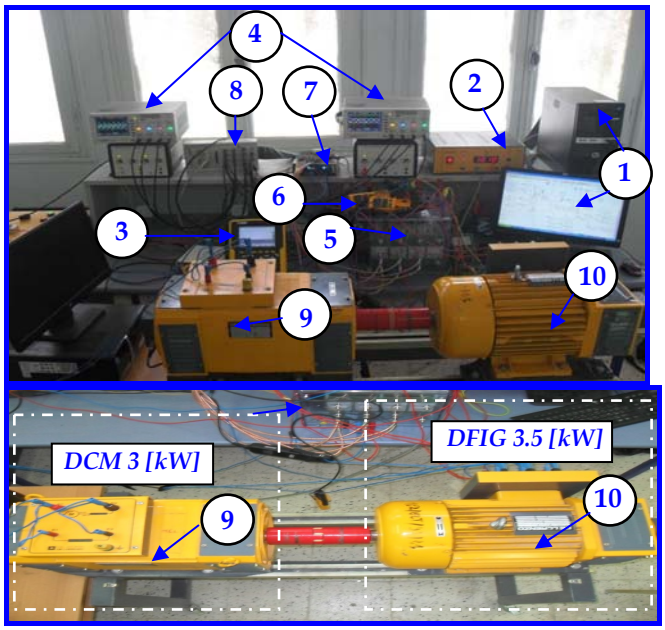

Fig. 5 – Experimental test bench (1 – PC, 2 – speed sensor, 3 – power analyzer, 4 – oscilloscopes, 5 – inverter (SEMIKRON), 6 – current sensors, 7 – voltage sensors, 8 – dSPACE1104, 9 – DCM, 10 – DFIG).

Figure 6 shows the hypo-synchronous mode, below the synchronous speed (< 1 500 rpm). It can be seen a proportionality between rotor speed and rotor currents in terms of rotor frequency. Figure 6a displays the speed increasing from 980 rpm to 1 480 rpm and then the speed decreasing with the same speed value (1 480 rpm to 980 rpm. Figure 6b presents only the speed increasing (from 900 rpm to 1 300 rpm) and the increasing period equal to 2 s. It clear that the rotor frequency is increasing f_r [Hz]. Figure 6c shows only the speed decreasing (from 1 050 to 700 rpm) and also the decreasing period equal to 2 s. It clear that the rotor frequency is decreasing f_r [Hz].

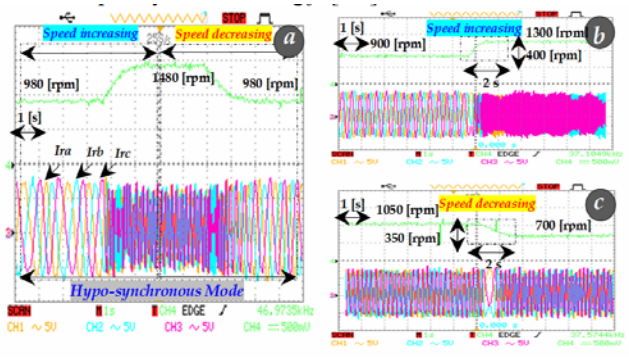

Fig. 6 – Rotor current and variation of rotor speed (hypo-synchronous mode).

Figure 7 presents the transient and steady states of rotor and stator currents with variation of rotor speed by action to the DCM, which produces a higher aerodynamic torque that means a lower wind velocity applied into the DFIG. In this case the rated speed is 1 420 rpm. Figure 7a presents a transient and steady states respectively of rotor currents and rotor speed, the transient state is applied from 0 s into 1 s, the rotor currents have sinusoidal form and lower frequency, and the rotor speed equal to 1 000 rpm. The steady state is applied from 1 s into 3 s, it can be seen the rotor frequency increasing due to the variation of the rotor speed. Figures 7b and Fig. 7c display the transient states respectively of rotor currents and rotor speed with another value equal to 500 rpm. Figures 7e present the transient and steady states respectively of stator currents which have the sinusoidal forms. Figures 7f shows the magnitude increasing of rotor currents from 3 to 5 A.

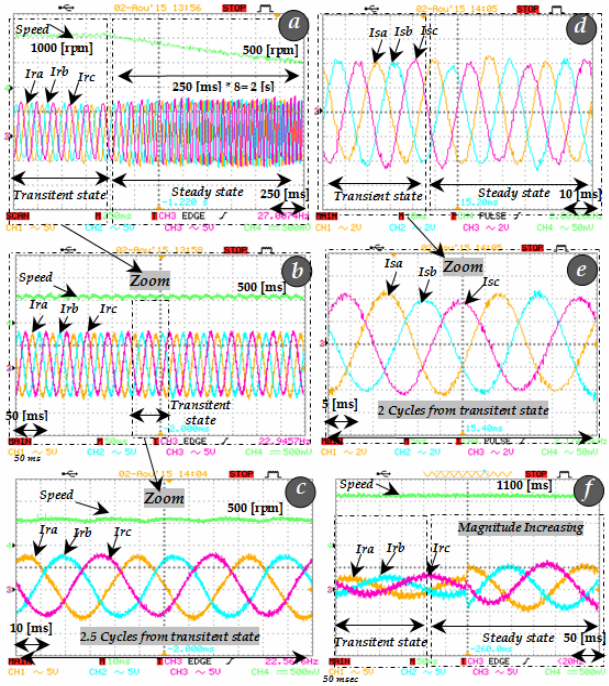

Fig. 7 – Transient and steady states of rotor and stator currents with variation of rotor speed.

Figures 8a and 8b present the transient and steady states respectively of magnitude increasing of rotor reference transversal current I^*_{rq}[A] from –7 A to –5 A , and the rotor reference direct current equals to 0 A . In Fig. 8b, it can be seen the good tracking of the measured current I_{rq_meas} [A] and few current error with a neglected overshoot. Also, the negative value of reference transversal current means a negative torque, this case is generator mode. Figures 8c shows the stator currents I_{s_abc}[A] and the stator voltage V_{sb} [A] , it is clear that the stator current I_{sb} [A] and stator voltage V_{sb} [V] are 180° out-off phase, which proves that only the active power flows to the grid (that means: the generator mode; which stator reactive power Q_s [var] equal to 0 var . Figures 8d, e and f display the rotor reference transversal current variation by applying a negative value (means negative torque C_e (N·m) from –7 A to –3 A (Figs. 8e and f), zero value applying to the reference direct current I^*_{rd} [A] to ensure exchange only the stator active power (Q_s = 0 var).

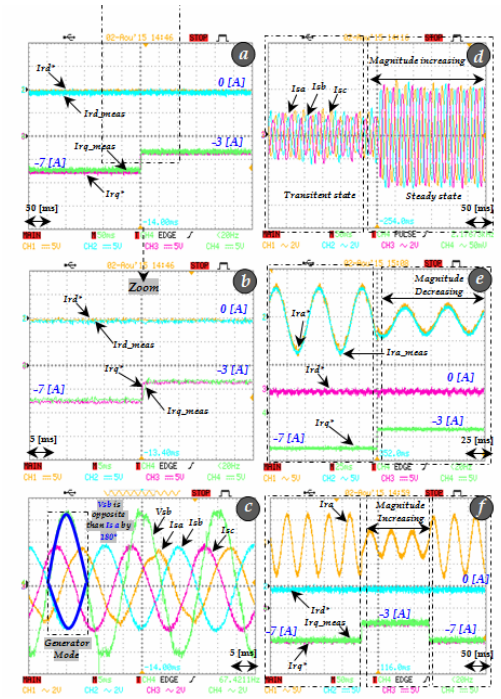

Fig. 8 – Tracking performance of rotor currents and the generator mode.

Figures 9 obtained from the power quality analyzer that shows the stator current THD (THD_I_{s_abc} [A]) equal to 3.7 %; less than 5 % satisfies the IEEE harmonic standard 519.

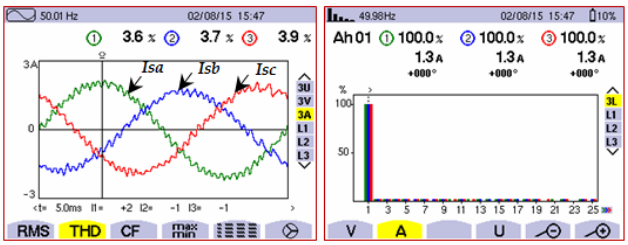

Fig. 9 – Experimental measures obtained from power quality analyzer (THD of stator currents).

Figure 10a displays steady state of the performance of reference direct current. It is clear that the rotor sinusoidal measured current I_{ra_meas} [A] follows exactly its reference I^*_{ra} [A]. By using the hysteresis current controller with hysteresis band equals $\Delta I = \pm 0.001$A this band is sufficient to follow the reference sinusoidal current. Figures 10b shows a simultaneity variation of reference direct and transversal currents, it can be seen a good tracking of measured current with a neglected overshoot. It can be seen also an exchange of stator active power by keeping zero value of reference direct current.

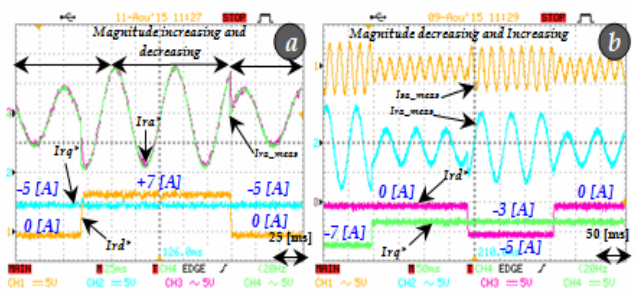

Fig. 10 – Robustness tests by variation of reference transversal current to ensure the unity power factor.

Table 1

Parameters of the DFIG

Rated power:	3.5 kW
Stator resistance:	Rs = 2.3 Ω
Rotor resistance:	Rr = 6.95 Ω
Stator inductance:	Ls = 0.04 H
Rotor inductance:	Lr = 0.036 H
Mutual inductance:	Lm = 0.061 H
Rated voltage:	Vs = 220/380 V
Number of pole pairs:	P= 2
Rated speed:	N = 1420 rpm
Friction coefficient:	fDFIG = 0.00 N.m/s
The moment of inertia	J = 0.2 kg.m^2

7. CONCLUSION

This paper presents the real time implementation of high performance FOC for a grid-connected doubly fed induction generator. The proposed approach is tested using an experimental test bench which consists from an emulator turbine represented by DCM and DFIG. The control strategy has been validated experimentally, the results obtained shows a good tracking of the predefined references regardless the wind speed changing. In this work, grid side converter (GSC) exchanges only active power with grid to guarantee unity power factor. The stator current injected into the grid have low total harmonic distortion (THD) equal to (3.7 %) satisfies the IEEE harmonic standard 519. The proposed method presents implementation and lower switching frequency converter. In future work, to improve the power quality, the DFIG will be used as an active filter.

Received on October 16, 2015

REFERENCES

1. Heng Nian, Yipeng Song, *Direct Power Control of Doubly Fed Induction Generator under Distorted Grid Voltage*, IEEE Transactions on Power Electronics, **29**, *2*, 2014.
2. Heng Nian, Peng Cheng, Z.Q. Zhu, *Coordinated Direct Power Control of DFIG System without Locked Loop under Unbalanced Grid Voltage Conditions*, IEEE Transactions on Power Electronics 2015.
3. Roberto Cárdenas, Rubén Peña, Salvador Alepuz, Greg Asher, *Overview of Control Systems for the Operation of DFIGs in Wind Energy Applications*, IEEE Transactions on Industrial Electronics, **60**, *7*, 2013.
4. Jafar Mohammadi, Sadegh Vaez-Zadeh, Saeed Afsharnia, Ehsan Daryabeigi. *A Combined Vector and Direct Power Control for DFIG-Based Wind Turbines*, IEEE Transactions on Sustainable Energy, **5**, *3*, 2014.
5. Michael K. Bourdoulis, Antonio T. Alexandridis, *Direct Power Control of DFIG Wind Systems Based on Nonlinear Modeling and Analysis*, IEEE Journal of Emerging and Selected Topics in Power Electronics, **2**, *4*, 2014.
6. Bhim Singh, N. K. Swami Naidu, *Direct Power Control of Single VSC-Based DFIG without Rotor Position Sensor*, IEEE Transactions on Industry Applications, **50**, *6*, 2014.
7. Jiefeng Hu, Jianguo Zhu, David G. Dorrell, *Predictive Direct Power Control of Doubly Fed Induction Generators Under Unbalanced Grid Voltage Conditions for Power Quality Improvement*, IEEE Transactions on Sustainable Energy, **6**, *3*, 2015.
8. Jiefeng Hu, Jianguo Zhu, David G, Dorrell, *Model-predictive direct power control of doubly-fed induction generators under unbalanced grid voltage conditions in wind energy applications*. IET Renewable Power Generation, **8**, pp. 687–695, 2014.
9. E.G. Shehata, *Sliding mode direct power control of RSC for DFIGs driven by variable speed wind turbines*, Alexandria Engineering Journal, 2015.
10. S. Taraft , D. Rekioua, D. Aouzellag, S. Bacha, *A proposed strategy for power optimization of a wind energy conversion system connected to the grid*. Energy Conversion and Management, 2015.
11. Badre Bossoufi, Mohammed Karim, Ahmed Lagrioui, Mohammed Taoussi, Aziz Derouich, *Observer backstepping control of DFIG-*

Generators for wind turbines variable-speed: FPGA-based implementation, Renewable Energy, 2015.

12 G. D. Marques and Matteo F. Iacchetti, *Stator Frequency Regulation in a Field-Oriented Controlled DFIG Connected to a DC Link*, IEEE Transactions on Industrial Electronics, **61**, *11*, pp. 5930–5939, 2014.

13. Matteo F. Iacchetti, Gil D. Marques, Roberto Perini, *A Scheme for the Power Control in a DFIG Connected to a DC Bus via a Diode Rectifier*, IEEE Transactions on Power Electronics, **30**, *3*, pp. 1286–1296, 2015.

14. P.K. Gayen, D. Chatterjee, S.K. Goswami, *Stator side active and reactive power control with improved rotor position and speed estimator of a grid connected DFIG (doubly-fed induction generator)*, Energy, 2015.

15. Rishabh Dev Shukla, Ramesh Kumar Tripathi, *Isolated Wind Power Supply System using Double-fed Induction Generator for remote areas*, Energy Conversion and Management, **96**, pp. 473–489, 2015.

16. Minh Quan Duong, Francesco Grimaccia, Sonia Leva, Marco Mussetta, Kim Hung Le, *Improving Transient Stability in a Grid-Connected Squirrel-Cage Induction Generator Wind Turbine System Using a Fuzzy Logic Controller*, Energies, **8**, pp. 6328–6349, 2015.

17. Fan Xiao, Zhe Zhang, Xianggen Yin, *Fault Current Characteristics of the DFIG under Asymmetrical Fault Conditions*, Energies, **8**, pp. 10971–10992, 2015.

18. Buja G.S., Kazmierkowski M.P., *Direct torque control of PWM inverter-fed AC motors-survey*, IEEE Transactions on Industrial Electronics, **51**, pp. 744–57, 2004.

19. Trzynadlowski A.M., *Scalar control methods*, *Control of induction motors* (Ch. 5), San Diego, Academic Press, pp. 93–105, 2001.

20. Mansour Mohseni, Syed M. Islam, Mohammad A.S. Masoum, *Enhanced Hysteresis-Based Current Regulators in Vector Control of DFIG Wind Turbines*, IEEE Transactions on Power Electronics, **26**, pp. 223–234, 2011.

21. Abdullah Asuhaimi, B. Mohd Zin, Mahmoud Pesaran H.A., Azhar B. Khairuddin, Leila Jahanshaloo, Omid Shariati, *An overview on doubly fed induction generators' controls and contributions to wind based electricity generation*, Renewable and Sustainable Energy Reviews, **27**, pp. 692–708, 2013.

22. AG. Abo-Khalil, G. Ahmed, *Synchronization of DFIG output voltage to utility grid in wind power system*, Renewable Energy, **44**, pp. 193–198, 2012.

23. G. Abad J. Lopez, M.A. Rodrıguez, L. Marroyo, G. Iwanski, *Doubly fed induction machine: modeling and control for wind energy generation*, IEEE press Series on Power Engineering, 2011.

24. Jiefeng Hu, Jianguo Zhu, David G. Dorrell, *Predictive Direct Power Control of Doubly Fed Induction Generators Under Unbalanced Grid Voltage Conditions for Power Quality Improvement*, IEEE Transactions on Sustainable Energy, **6**, *3*, pp. 943– 950, 2015.

25. M.K. Mishra, K. Karthikeyan, *An Investigation on Design and Switching Dynamics of a Voltage Source Inverter to Compensate Unbalanced and Nonlinear Loads*, IEEE Transaction, on Industrial Electronics, **56**, *8*, pp. 2802–2810, 2009.

26. Ali Chebabhi, Mohammed-Karim Fellah, Mohamed-Fouad Benkhoris, *3d Space Vector Modulation Control Of Four-Leg Shunt Active Power Filter Using Pq0 Theory*, Rev. Roum. Sci. Techn. – Électrotechn. et Énerg., **60**, *2*, pp. 185–194, 2015.

27. Tarak Benslimane, *Open Switch Faults Detection and Localization in Three Phases Shunt Active Power Filter*, Rev. Roum. Sci. Techn.– Électrotechn. et Énerg., **52**, *3*, pp. 359–370, 2007.